Comprehensive Characterization of Soft Tissue and Surrogate Materials Across Varied Loading Methods

C. J. Dennis[1], and C. E. Quenneville[1]
[1] McMaster University

ABSTRACT

Exploring the mechanical properties of soft tissues under compressive loading is crucial for understanding their role in automobile incidents. Soft tissues, which serve as cushions or padding between bone and vehicle interiors, significantly influence contact duration and forces, thereby altering incident kinematics and injury. In this investigation, muscle, and soft connective tissues from post-mortem human subjects (PMHS) forearms were excised and subjected to compression and indentation testing methods at various rates and strains. Specific samples with higher proportions of muscle were compared against samples without muscle tissues to evaluate how the role of compositional changes. Anthropomorphic Test Device (ATD) upper extremity foam and vinyl-foam composite analog tissues underwent similar testing for comparison. High impact rates simulating those in high-speed automotive collisions were achieved using a custom-built drop tower impactor setup. The results revealed significantly higher stiffness values for samples with large proportions of muscle tissue compared to no muscle samples at smaller deformations. Substantial differences in stiffness were seen between soft tissues and ATD materials across most loading rates and strains, although some exceptions were noted at higher rates and strains. An indentation and modified Zener model were used to quantify material parameters. These findings provide a solid basis for advancing ATD analogs and have broader implications for soft tissue research. Moreover, this work represents a crucial step towards enhancing safety standards in the automotive industry.

INTRODUCTION

Historically, automotive injury prevention research has focused on the head and torso. Due to increased protection from seatbelts and airbags, the upper and lower extremities are now dominant injury locations (Forman et al., 2015). The majority of upper extremity injuries from automotive collisions occur to the forearm, most commonly in the form of a fracture (Forman et al., 2015; Frampton et al., 1997). These injuries are caused by the forearm being forcefully propelled into a rigid object, either from the collision itself or triggered by airbag deployment (Duma et al., 2002; Jernigan et al., 2005). They can also occur from the airbag itself, depending on forearm positioning relative to the steering wheel (Forman et al., 2015; Pintar & Yoganandan, 2002).

In industry, Anthropomorphic Test Devices (ATDs) are used to assess the injury risk to different body regions (Mitchell et al., 2013). Equipped with sophisticated instrumentation, data

This paper is a student paper from the 19th Injury Biomechanics Symposium and is published in a special issue of SAE International Journal of Transportation Safety.
It is preliminary work, has not been peer reviewed, and should not be cited because it is a work in progress.

are gathered during collision tests, which can then be compared to injury limits derived from controlled lab settings (Crandall et al., 2011; Mitchell et al., 2013). Impact loads applied to the exterior of the body transmit load to the metallic ATD 'skeleton' (where instrumentation is located) through their soft tissue analog, where the energy attenuation depends on its modulus (Crandall et al., 2011; Mitchell et al., 2013), which affects the contact duration and resulting forces. However, there remains limited data regarding the specific properties this flesh analog requires to replicate real-world responses accurately.

To define target material properties, tissue may be tested either *in vivo* or *ex vivo*. Testing *in vivo* has been limited to ensure no injury to participants, and as such does not provide adequate information relevant to large strain, high rate loading. For *ex vivo* testing, post-mortem human subjects (PMHS) are considered the most anatomically accurate representation of *in vivo* response (Chanda, 2018; Mitchell et al., 2013). Samples can be tested either *in situ* or extracted, at a range of rates and to destructive levels (Comley & Fleck, 2009; Sun, Gepner, et al., 2021; Sun, Lee, et al., 2021; Van Sligtenhorst et al., 2006), facilitating quantification of material elastic modulus.

Several challenges with PMHS may affect measured properties, such as dehydration (Ward & Lieber, 2005), time post-mortem (Böl et al., 2016), consistency in sample dimensioning (Böl et al., 2012), freeze-thaw cycling (Gottsauner-Wolf et al., 1995), and age (Agache et al., 1980). Variations in test setups through the literature, compounded by natural inter-subject variability, have precluded a consensus on tissue properties. Perhaps one of the most important physiological properties missing in PMHS tissues is muscle activation, as it has been shown in volunteer-based studies that stiffness can increase two-fold when muscles are activated (Bosnic et al., 2022; Shinohara et al., 2010). During anticipated collisions occupants typically brace before impact, and as such passive muscle (relaxed) has been considered to represent unanticipated collisions, such as in distracted driving scenarios (Mitchell et al., 2013).

Traditionally, research has focused on measuring the bulk properties of soft tissues; however, attention has shifted to a more nuanced approach that considers the composition of tissues (*i.e.* muscle, adipose, skin) (Gefen & Haberman, 2007; Hendriks et al., 2003; Shoham & Gefen, 2016). Within the forearm by location, and across individuals of varying body types, these distributions vary widely, and as such an effort must be made to characterize each tissue type individually to properly identify the role each tissue plays in impact attenuation properties.

The overall objective of this work was threefold: first, to characterize forearm soft tissue response to compressive loading *ex vivo* over a range of rates relevant to automotive collisions using indentation and unconfined compression. Second, was to assess how the combination of muscle and adipose tissues affected these properties, and third, was to compare to current ATD soft tissue analog materials to inform future biofidelic material development.

METHODS

Sample Preparation

Six PMHS arm pairs were obtained (male, age 72±9 years, body mass 84.6±5.1 kg, stature 176.5±4.4 cm, BMI 27.3±2.9). For each forearm, three core samples and one cubic sample of soft tissue were extracted from the anterior and posterior aspects of the forearm midpoint (total n=36

This paper is a student paper from the 19th Injury Biomechanics Symposium and is published in a special issue of SAE International Journal of Transportation Safety.
It is preliminary work, has not been peer reviewed, and should not be cited because it is a work in progress.

cores, n=12 cubes). Core samples were extracted using a custom-made rig consisting of an 8mm diameter coring tool (Alabama Specialty Products Inc., AL) mounted to a handheld drill guide (Milescraft, DrillMate). Cube samples were manually excised with a scalpel to a target size of 20mm x 20mm x 10mm (L x W x H). Samples were excised while frozen and then returned to the freezer until testing, at which point samples were thawed in phosphate buffer saline (PBS) at room temperature for at least one hour. Initial tissue thickness was measured for each sample, along with proportions of skin/muscle/adipose.

Current ATD soft tissue analogs were obtained for the Hybrid III and THOR ATDs (Humanetics Group, MI, USA). The surrogates were made from the same material that is used in the forearm region of the ATDs in two forms: foam, and a sandwich of foam encased in vinyl. The vinyl-foam composite had ~2mm thick vinyl walls surrounding the inner foam material. Both were produced in 15mm thick sheets and cut to match the geometry of the cubic samples (Figure 1).

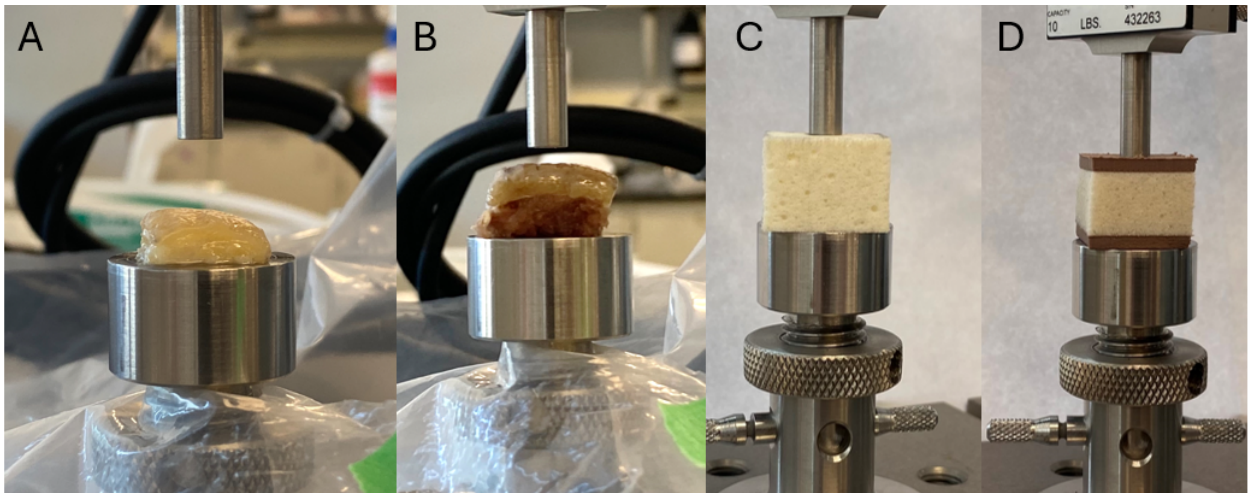

Figure 1: Indentation setup for PMHS and ATD samples.
All images depict an indentation setup on the materials testing machine. (A) PMHS sample composed of just adipose and skin, (B) PMHS sample composed of skin, adipose, and muscle, (C) ATD foam sample, and (D) ATD foam-vinyl composite sample.

Unconfined Compression

Samples were tested at a quasi-static strain rate ($0.01s^{-1}$), a moderate strain rate ($1s^{-1}$), and a high strain rate ($200s^{-1}$) to encompass the range expected during automotive collisions (Van Loocke et al., 2009).

For the quasi-static and moderate strain rates, one core sample from each donor was tested at each rate using an ElectroPuls E1000 material testing machine (Instron, MA, USA) instrumented with a 250N load cell with an accuracy of ± 1.25N. Loads were applied to samples via platens (Figure 2). Each sample received 12 preconditioning cycles (20% strain, at a rate of $0.01s^{-1}$), a 3-minute recovery period, followed by a data collection cycle (50% strain at required rate). Due to thickness variability, loading rate was customized for each sample to achieve the target strain rate.

This paper is a student paper from the 19th Injury Biomechanics Symposium and is published in a special issue of SAE International Journal of Transportation Safety.
It is preliminary work, has not been peer reviewed, and should not be cited because it is a work in progress.

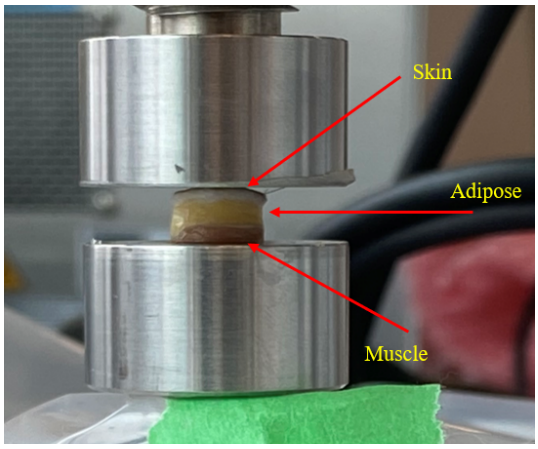

Figure 2: Unconfined compression setup.
Each PMHS core sample was tested in unconfined compression on the materials testing machine, with the tissue components (skin, adipose, and muscle) indicated.

As the high strain rate exceeded the capacity of the material testing machine, a custom drop tower was constructed (Figure 3). The drop mass (1.26 kg) was guided along linear rails to achieve an impact speed of 2.0 m/s. Samples were compressed to a maximum 50% strain (restricted by two adjustable stoppers on either side of the sample). Force data were acquired using a 100lb quartz ICP force ring sensor (PCB 201B02, PCB Piezotronics Inc., NY, USA, 90kHz sampling rate). A high-speed camera (MotionXtra NX3S1, Velocity Dynamics, BC, Canada) was positioned to capture the sample deformation (recorded at 1250 fps). One cubic sample from each specimen was tested.

This paper is a student paper from the 19th Injury Biomechanics Symposium and is published in a special issue of SAE International Journal of Transportation Safety.
It is preliminary work, has not been peer reviewed, and should not be cited because it is a work in progress.

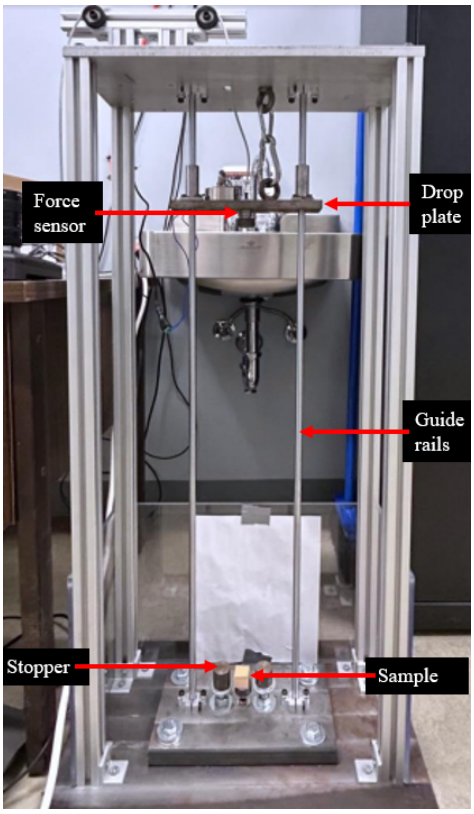

Figure 3: Custom-built drop tower for high rate testing.
Samples were placed at the bottom of a custom-built drop tower, where force during impact was measured with a force sensor, and the strain was limited using adjustable stoppers.

Indentation Testing

One cubic sample from each specimen was tested at each strain rate (quasi-static, $0.01s^{-1}$ and moderate, $1s^{-1}$); high rate was not conducted due to equipment limitations. All testing was conducted with the same material testing machine, now instrumented with a 44N in-line load cell (MLP-10, A-Tech Instruments Ltd., ON, Canada) with an accuracy of ±0.01N. Loads were applied to the center of each cubic sample via a 6mm diameter flat-ended cylindrical indenter.

Each sample received 12 preconditioning cycles (20% strain, at a rate of $0.01s^{-1}$), a 3-minute recovery period, followed by a data collection cycle (20% strain at required rate). Loading rate was customized for each sample to achieve the target strain rate.

Data Analysis and Modelling

Unconfined Compression. Force-deformation data from each test were converted to stress-strain based on the sample's specific geometry. Data were modeled using a tri-linear elastic fit, where the modulus was calculated over specific deformation zones: E1 between 10-20% deformation, E2 between 20-30% deformation, and E3 was above 30% (to approx. 50%). All values were compared using a t-test with $\alpha = 0.05$.

This paper is a student paper from the 19th Injury Biomechanics Symposium and is published in a special issue of SAE International Journal of Transportation Safety.
It is preliminary work, has not been peer reviewed, and should not be cited because it is a work in progress.

Zener Modeling. A modified Zener model (Garcia et al., 2008) was also applied to the unconfined compression data using custom MATLAB code, representing the tissue as two linear springs (K1 and K2) and a linear dashpot (C) connected in parallel (**Error! Reference source not found.**). The modified version permits a deformation interval where K1 acts in isolation up to point Xs, after which K2 and C begin to act, which allows representation of non-linear characteristics of soft tissues. The best fit was determined based on minimizing overall R^2 for both compression intervals.

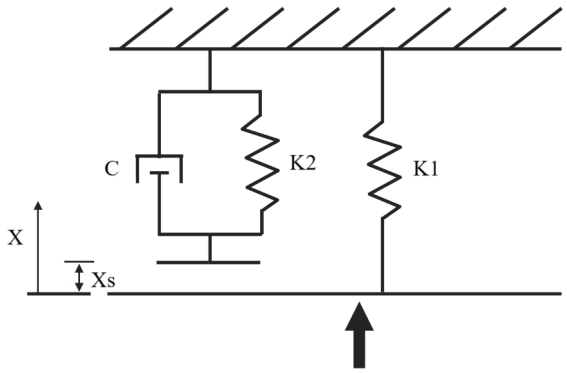

Figure 4: Modified Zener Model.
The modified Zener model used in this study included a critical displacement point X_s beyond which the additional linear spring and damper affected loading.

Indentation. Force-displacement data were used to calculate the indentation stiffness (S) from each test. Two models were then employed to obtain the "effective" elastic modulus. Indentation model 1 (IM1) used indenter radius (a) and a geometric correction factor (k) to calculate E*:

$$E^*=S/2ak \quad \text{(Eq.1)}$$

The k value was linearly extrapolated from previous work to account for the deformation in this study (Zhang et al., 1997). The second indentation model (IM2) used the same equation but was simplified to exclude the correction factor (k) (Oliver & Pharr, 1992).

RESULTS

Samples

Core sample heights and diameters were highly consistent when extracted from the same location but were affected by anatomical side. Anterior samples had a height of 7.9 ± 2.7 mm (mean ± SD), significantly higher than posterior ones (6.0 ± 1.9 mm, $p < 0.05$). Cube samples were prepared using a scalpel and 3D-printed jigs and thus had strong height consistency, 9.6 ± 1.8mm.

The impact of thawing on percentage changes in skin, adipose tissue, muscle, and total volume was assessed across core and cube samples (Table 1). All samples had a decrease in height

This paper is a student paper from the 19th Injury Biomechanics Symposium and is published in a special issue of SAE International Journal of Transportation Safety.
It is preliminary work, has not been peer reviewed, and should not be cited because it is a work in progress.

of 10-12% when thawed. This was overall evenly split between muscle and adipose tissues, as skin was largely unaffected by thawing.

Table 1: Frozen to thawed sample compositions
Height of individual tissue components for frozen and thawed states, all units in mm and are reported as mean ± S.D.

	Core Samples				**Cube Samples**			
	Skin	Adipose	Muscle	Total Height	Skin	Adipose	Muscle	Total Height
Frozen	0.9 ± 0.3	2.8 ± 2.3	3.9 ± 1.4	7.6 ± 1.9	1.2 ± 0.3	3.2 ± 2.2	5.2 ± 1.7	9.6 ± 1.8
Thawed	1.0 ± 0.3	2.5 ± 1.9	3.1 ± 1.5	6.6 ± 1.6	1.2 ± 0.4	2.8 ± 0.9	4.4 ± 1.3	8.4 ± 1.4

Core samples were grouped according to the proportion of muscle vs adipose, where 40-60% of their distribution due to muscle (n=6) was termed ‘muscle’ and those with 0% (n=4) were termed ‘non-muscle’.

Unconfined Compression

For the soft tissue high rate tests, an initial strain rate of ~$210s^{-1}$ was achieved, confirmed by high-speed video analysis. Elastic moduli were calculated for quasi-static (n=6), moderate-(n=6), and high rate (n=10) stress-strain curves in 10% strain increments, up to 50% total strain. At all stages, the high rate had statistically higher moduli than both moderate and quasi-static tests ($p < 0.05$). Moderate strain rates had higher moduli than quasi-static at 20%, 30%, and 40% strain levels ($p < 0.032$), but not at 10% or 50% ($p > 0.134$).

The ATD foam was less rate-dependent, with no significant differences observed between quasi-static and moderate rates ($p > 0.113$). However, the high rate modulus was significantly higher for all strains 20% and above ($p < 0.017$). The ATD vinyl-foam composite displayed more rate-dependent behavior, where differences were observed among all rates, except for 10% strains between quasi and moderate rates ($p = 0.10$), and between high rate and both quasi-static and moderate modulus values at 10% and 20% strains ($p > 0.15$).

Tri-linear elastic model. Statistically significant differences in soft tissue modulus values were observed among all three testing rates for all three strain intervals ($p < 0.05$). The ‘muscle’ and ‘no muscle’ results were compared for quasi-static and moderate rates, but not for high rates due to a lack of sample size in the no muscle group (n=1). Samples with muscle content generally had higher modulus values at both strain rates and all strain levels than their no muscle counterparts (Figure 5:Figure 5). These differences were statistically significant for E1 and E2 but did not reach significance for large strains (E3, $p = 0.15$).

This paper is a student paper from the 19th Injury Biomechanics Symposium and is published in a special issue of SAE International Journal of Transportation Safety.
It is preliminary work, has not been peer reviewed, and should not be cited because it is a work in progress.

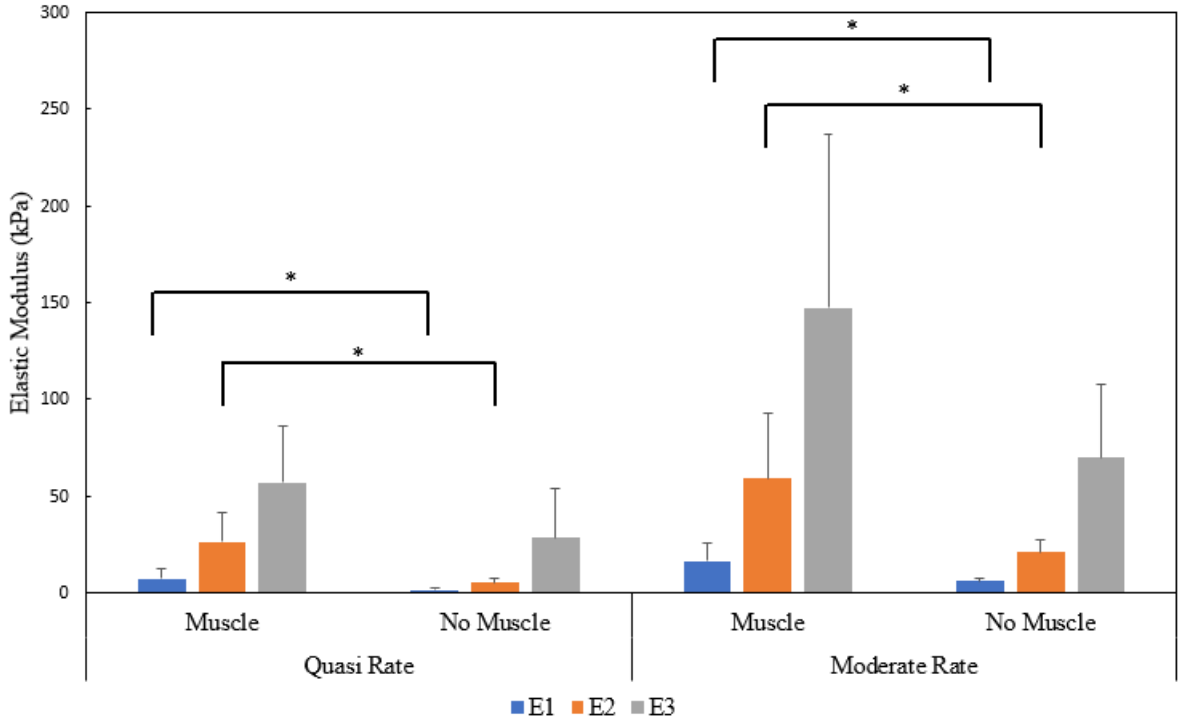

Figure 5: Effect of muscle content on modulus.
Samples with no muscle content were compared to those with 40-60% of their total tissue distribution attributable to muscle tissue. Asterisks (*) represent statistically significant differences between the muscle and non-muscle counterparts ($p < 0.05$).

When comparing ATD materials to PMHS tissues (all compositions combined), the vinyl-foam composite had higher E1, E2, and E3 values at all rates ($p < 0.05$ for all except E3 at high strain rate, $p = 0.07$). The foam material also had generally higher E1, E2, and E3, but this difference was not significant at certain strains and rates (E2 at high rate and E3 and moderate and high rate, $p > 0.05$) (

This paper is a student paper from the 19th Injury Biomechanics Symposium and is published in a special issue of SAE International Journal of Transportation Safety.
It is preliminary work, has not been peer reviewed, and should not be cited because it is a work in progress.

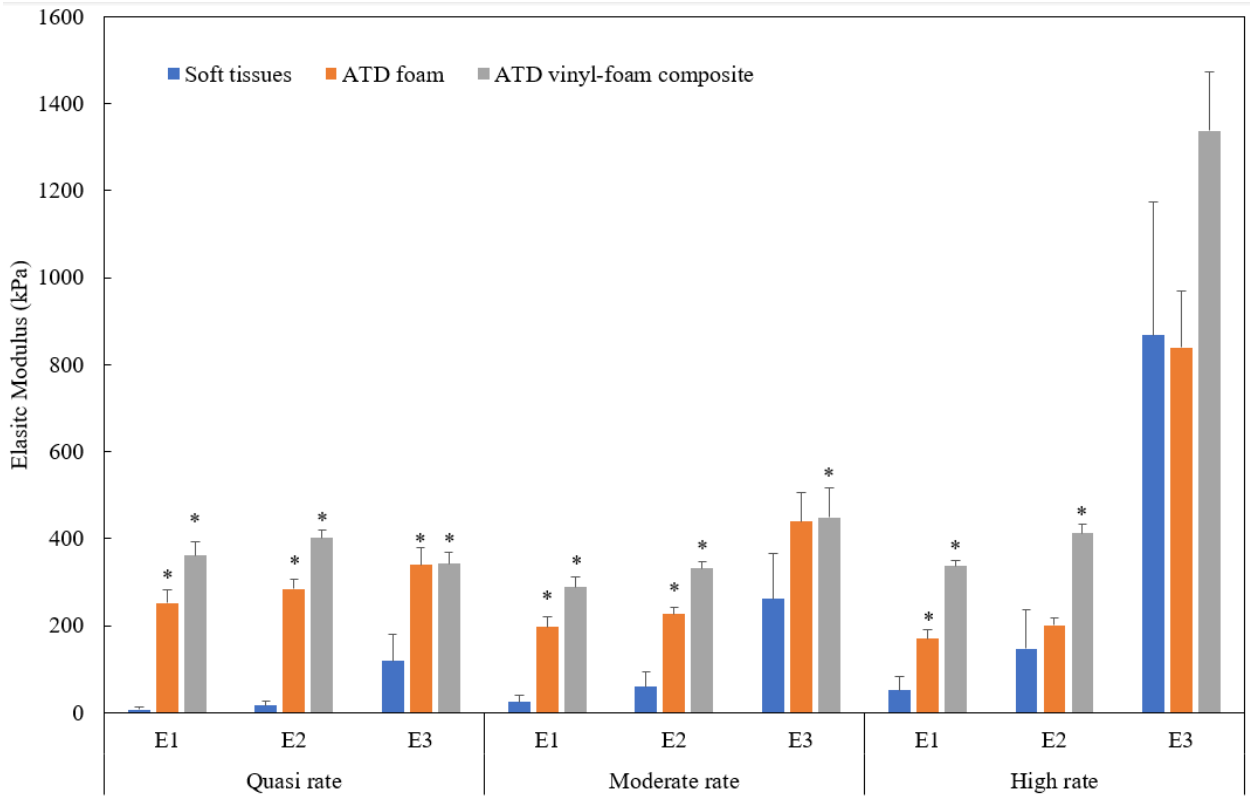

Figure 6).

This paper is a student paper from the 19th Injury Biomechanics Symposium and is published in a special issue of SAE International Journal of Transportation Safety.
It is preliminary work, has not been peer reviewed, and should not be cited because it is a work in progress.

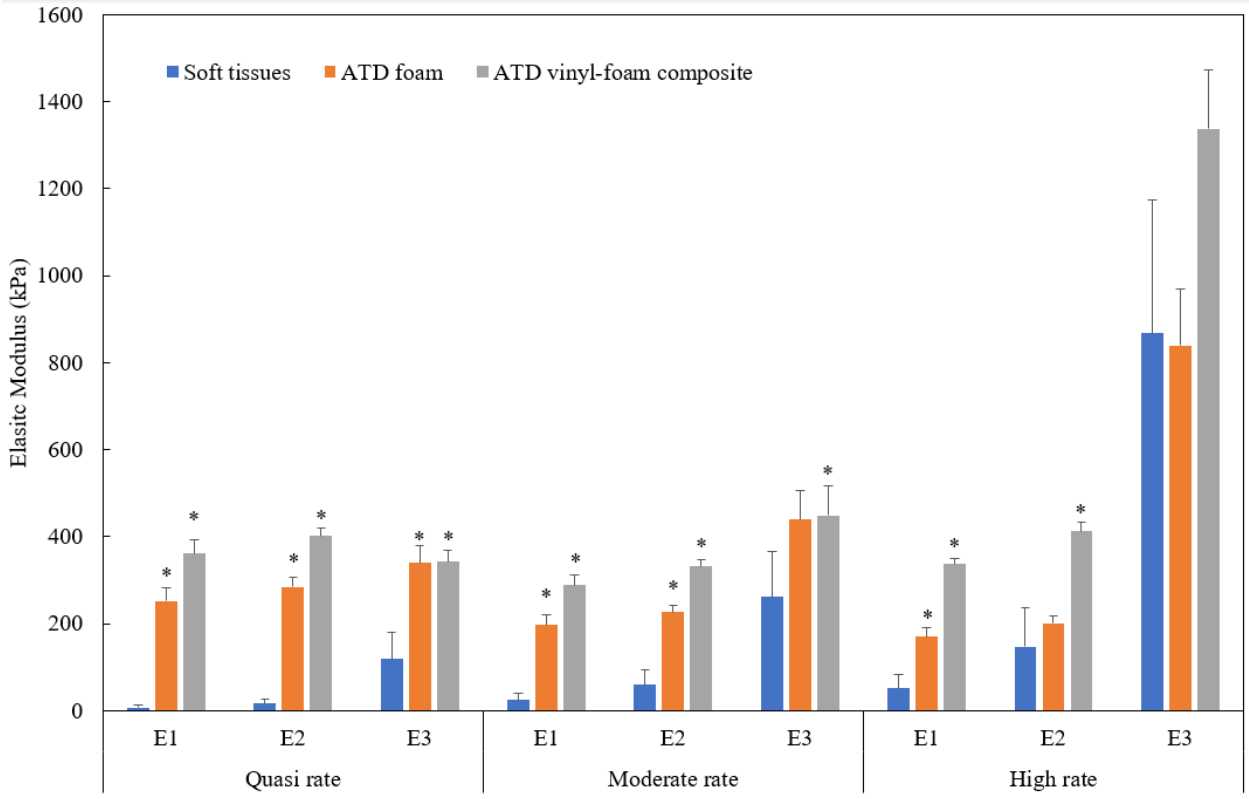

Figure 6: Tri-linear fit values for soft tissues, ATD foam, and ATD vinyl-foam composite materials at the three strain rates and for the three levels of strain (E1, E2, and E3). Asterisk (*) denotes a significant difference ($p < 0.05$) between the ATD analog and soft tissues.

Modified Zener Model

K1 values displayed the general trend of increasing as the strain rate increased, with statistically significant differences being found among quasi-static, moderate, and high rate K1 values. This same trend was also observed with the K2 values; however, with ATD foam samples the K2 value was near zero in all cases for quasi-static and moderate rates (non-zero for high rate). The dampening coefficient C displayed relative consistency among soft tissue samples, but again with ATD foam and ATD vinyl-foam composites, the model exhibited low values at quasi-static and moderate rates (Table 2).

This paper is a student paper from the 19th Injury Biomechanics Symposium and is published in a special issue of SAE International Journal of Transportation Safety.
It is preliminary work, has not been peer reviewed, and should not be cited because it is a work in progress.

Table 2: Zener model parameters
Zener model obtained parameters for soft tissues (ST), ATD foam, and ATD vinyl-foam composite (ATD comp) materials and their respective strain rates. Xs values are in strain, C values are in Ns/m, K1 and K2 values in N/m. All values are reported as mean ± S.D.

	Xs	**C**	**K1**	**K2**
ST quasi-static	0.27 ± 0.05	3.7 ± 3.5	11.8 ± 7.5	113.3 ± 60.5
ST moderate	0.30 ± 0.10	23.6 ± 15.1	27.6 ± 15.5	174.7 ± 74.7
ST high	0.36 ± 0.05	73.2 ± 48.8	61.7 ± 30.2	303.0 ± 173.8
ATD foam quasi-static	0.14 ± 0.14	2.4 E-12 ± 4.2 E-12	249.6 ± 13.4	3.68E-13 ± 5.73E-13
ATD foam moderate	0.14 ± 0.12	3.3 E-11 ± 5.7 E-11	297.1 ± 39.5	1.2 E-13 ± 1.4E-13
ATD foam high	0.42 ± 0.01	126.4 ± 81.2	967.5 ± 168.5	1473.3 ± 211.7
ATD comp quasi-static	0.3 ± 0.0	1.5E-6 ± 7.6E-07	305.4 ± 21.1	257.7 ± 38.9
ATD comp moderate	0.28 ± 0.01	2.8E-7 ± 2.9E-7	358.5 ± 15.5	353.9 ± 51.6
ATD comp high	0.38 ± 0.01	56.2 ± 7.1	1403.7 ± 314.7	8229 ± 1869

Indentation Modeling

The indentation model values and unconfined compression values (n=10) were compared such that the "effective" modulus would show agreement with the unconfined compression modulus if it was an accurate model. Two-tailed t-tests were used to compare indentation model 1 (IM1) & indentation model 2 (IM2) with the corresponding unconfined compression modulus values. IM1 resulted in statistically significantly lower modulus values than the unconfined compression modulus for both strain rates ($p < 0.009$). IM2 was considerably better, with no statistically significant differences between the "effective" modulus and the unconfined compression modulus for both quasi-static and moderate strain rates ($p = 0.59$). The ATD foam and vinyl-foam composite exhibited statistically significant higher modulus values than the soft tissue samples across all modulus values; however, the IM2 showed more agreement between its "effective" modulus and unconfined moduli for the vinyl-foam composite material than the foam.

DISCUSSION

This work presents the first known study that performed compressive materials characterization of PMHS soft tissues, Hybrid III, and THOR-50M surrogate materials over a wide range of loading rates. This work also showed the substantial effects of adipose/muscle compositions on measured properties. Due to the limited research available regarding these materials, these data are most valuable. Although these tests were done on materials obtained from the upper extremity, the findings may translate beyond this region throughout the body, due to the

This paper is a student paper from the 19th Injury Biomechanics Symposium and is published in a special issue of SAE International Journal of Transportation Safety.
It is preliminary work, has not been peer reviewed, and should not be cited because it is a work in progress.

consistent hierarchal structure of skin, adipose, and muscle, as well as for ATD surrogate materials as they are generally constant throughout the body, with thickness changing.

PMHS tissues provide the most anatomically accurate representation of human responses at large strains. However, limitations such as lack of muscle activation, alteration of characteristics due to freezing, or tissue hydration must be acknowledged. Steps were taken in the present work in an attempt to limit these effects by only having one freeze-thaw cycle and submerging tissues in phosphate-buffered saline before testing (Ward & Lieber, 2005);. The lack of muscle activation remains but is consistent with the field and is in line with how ATD validation is typically done. Additionally, this passive tissue response would represent unanticipated collisions, where minimal bracing response occurs.

Coring soft tissue samples offers a precise and efficient method for obtaining consistent sample diameters across multiple specimens. Normally, these samples are acquired using a biopsy punch tool, which cuts by pushing the tool into the tissue. The coring tool presented herein uses rotation to drive the cutting process, which circumvents potential "ballooning" that may occur with the traditional punch approach. This resulted in samples with well-defined edges, facilitating consistent cross-area for stress calculations, which was aided by removal while the tissue was frozen. Cube samples were also removed in the present work using a scalpel, which is the standard for *ex-vivo* studies, but is user-dependent which makes consistency among samples more difficult. This was addressed via the use of 3D printed jigs, to make the sample size more standardized.

Substantial volumetric changes were observed during the thawing process, which contrasts with previous work (Leonard et al., 2022). One reason for this change may be that because the samples were excised, they no longer had surrounding tissue to support their shape. This could also be attributed to the high water content of adipose and muscle tissues. Furthermore, the previous study was conducted on rabbit muscle tissue (in contrast to the present human PMHS study). Determination of displacement rates in future work should thus be based on measurements taken post-thaw to ensure strain rates are consistent and accurate.

Muscle and non-muscle elastic moduli were compared at quasi-static and moderate rates. For smaller deformations (<30% strain) muscle samples had significantly higher moduli than the no-muscle group. While the difference at large deformations was not significant, this was likely due to the large standard deviation observed, and additional samples may reach significance. High rate tests were also absent in this evaluation for the same reason, as only one cubic sample had no muscle tissue. Moving forward, it would be worthwhile to further explore both these areas to get a better understanding of the role of tissue composition in compressive loading scenarios. Considering that the muscle content had higher modulus values it might be worthwhile exploring how exclusively muscle samples and ATD materials compare.

Unconfined compression is a mainstay method for characterizing material properties. Soft tissues showed an increase in elastic modulus with increasing strain rates, as was expected of viscoelastic biomaterials. The quasi-static, moderate, and high strain rates were selected to highlight the strain rate dependence of the materials, with the high rate reflecting rates reported in automobile collisions (Van Loocke et al., 2009). The maximum strain of 50% was selected based on that which was used in previous soft tissue studies (Commisso et al., 2016; Miller-Young et al., 2002).

The study used a tri-linear fit to represent the elastic moduli of soft tissues. The initial 0-10% strain data was not included in the fit due to the substantial compliance of the soft tissues in this initial range. The 10-20% (E1) and 20-30% (E2) increments were chosen to encompass similar

This paper is a student paper from the 19th Injury Biomechanics Symposium and is published in a special issue of SAE International Journal of Transportation Safety.
It is preliminary work, has not been peer reviewed, and should not be cited because it is a work in progress.

data ranges, and the 30-50% range of E3 was chosen due to the rapid increase in stress observed from this strain onwards. There was a large change in modulus over E3 in particular, and as such dividing into smaller increments in the future may provide greater insight into tissue responses at these higher deformations.

Indentation studies help evaluate the role of surrounding tissues on material characteristics, while also allowing easy experimental setup where the key components are the indentation probe and sample geometry. IM2 successfully modeled soft tissue response, to the extent that no differences were identified between the calculated "effective" modulus and the unconfined compression modulus at both quasi and moderate strain rates. Notably, high rate testing was missing from the indentation methods; this was due to the instrumentation setup, where high rate tests would have exceeded the capacity of the in-line force sensor and may be addressed in future work.

The Zener model was chosen to model the soft tissues' viscoelastic behaviors with its spring (elastic) and dashpot (viscous) elements. The model was selected due to its mathematical ease of use and the ability to add more parameters should it prove ineffective in modeling the non-linear viscoelastic behavior of soft tissues. Overall, the Zener model fit the soft tissue data well. Zener models have been applied previously to soft tissues (Chawla et al., 2009), but typically with much lower K1 values (*e.g.* 27.6 and 29.8 kPa) but this could be attributed to these prior studies being exclusively muscle tissue.

An ATD soft tissue analog must represent real tissues across a range of speeds and deformations. In unconfined compression, both ATD foam and vinyl-foam materials showed significantly higher moduli than the soft tissues. The ATD materials also displayed a plastic plateau from 20-40% strain before stiffening. When compared to the soft tissues using the tri-linear fit, higher moduli were found for nearly all strains and rates. These findings demonstrated that at most points the ATD materials are significantly stiffer than the soft tissues, yet tend to improve as strains and loading rates get larger. This suggests that ATD materials may exhibit biofidelic characteristics in high-loading scenarios.

Designing an ATD surrogate involves a complex interplay of factors, each crucial to its effectiveness. Durability stands as a paramount concern, ensuring repeated and consistent use without compromising accuracy. However, this often stands in conflict with biofidelity. Creating a completely biofidelic soft tissue analog within current constraints may be unattainable. From the work presented herein, currently, the ATD foam displays more similar characteristics to that of the soft tissue, yet it may lack the necessary durability needed for repeated use. A composite with reduced stiffness (thinner vinyl, or softer foam) or materials specifically designed to reflect the individual soft tissue components (adipose and muscle) may better address the competing priorities with a more realistic response.

This work established essential target parameters that alternate technologies, such as 3D printing, could use to develop more realistic and functional ATD materials. By focusing on these target parameters, future iterations of ATD surrogates can achieve improved compressive accuracy in crash tests.

This paper is a student paper from the 19th Injury Biomechanics Symposium and is published in a special issue of SAE International Journal of Transportation Safety.
It is preliminary work, has not been peer reviewed, and should not be cited because it is a work in progress.

CONCLUSIONS

Soft tissues mitigate forces experienced in different loading situations, such as automobile collisions. Historically, obtaining mechanical properties of tissues in such scenarios posed challenges due to the absence of standardized methodologies and difficulties in acquiring tissue samples.

This work characterized and modeled soft tissues under compressive loading across varying strains and loading rates, which not only enriches our understanding of tissue behavior but also holds significant implications for safety considerations in various fields. Current ATD materials have demonstrated relevance in specific contexts; however, they tend to be overly stiff when contrasted with soft tissues due to durability requirements.

These data set the stage for future advancements in developing more biofidelic surrogates, which can thus be used to ensure improved safety standards and enhanced biomechanical models, crucial for mitigating injuries in automobile and other impact scenarios.

ACKNOWLEDGEMENTS

This work recognizes the contributions of the anatomical donors, as well as Humanetics for providing the ATD analog materials used herein.

REFERENCES

Agache, P. G., Monneur, C., Leveque, J. L., & De Rigal, J. (1980). Mechanical properties and Young's modulus of human skin in vivo. *Archives of Dermatological Research*, *269*(3), 221–232. https://doi.org/10.1007/BF00406415

Böl, M., Kruse, R., Ehret, A. E., Leichsenring, K., & Siebert, T. (2012). Compressive properties of passive skeletal muscle-The impact of precise sample geometry on parameter identification in inverse finite element analysis. *Journal of Biomechanics*, *45*(15), 2673–2679. https://doi.org/10.1016/j.jbiomech.2012.08.023

Böl, M., Leichsenring, K., Ernst, M., & Ehret, A. E. (2016). Long-term mechanical behaviour of skeletal muscle tissue in semi-confined compression experiments. *Journal of the Mechanical Behavior of Biomedical Materials*, *63*, 115–124. https://doi.org/10.1016/j.jmbbm.2016.06.012

Bosnic, M., Rasoulian, A., & Brandon, S. C. E. (2022). Investigating the effects of activation state and location on lower limb tissue stiffness. *Journal of Biomechanics*, *135*, 111032. https://doi.org/10.1016/j.jbiomech.2022.111032

Chanda, A. (2018). Biomechanical modeling of human skin tissue surrogates. *Biomimetics*, *3*(3). https://doi.org/10.3390/biomimetics3030018

Chawla, A., Mukherjee, S., & Karthikeyan, B. (2009). Characterization of human passive muscles for impact loads using genetic algorithm and inverse finite element methods. *Biomechanics and Modeling in Mechanobiology*, *8*(1), 67–76. https://doi.org/10.1007/s10237-008-0121-6

Comley, K., & Fleck, N. A. (2009). The high strain rate response of adipose tissue. *IUTAM*

This paper is a student paper from the 19th Injury Biomechanics Symposium and is published in a special issue of SAE International Journal of Transportation Safety.
It is preliminary work, has not been peer reviewed, and should not be cited because it is a work in progress.

Bookseries, *12*, 27–33. https://doi.org/10.1007/978-1-4020-9404-0_4
Commisso, M. S., Calvo-Gallego, J. L., Mayo, J., Tanaka, E., & Martínez-Reina, J. (2016). Quasi-Linear Viscoelastic Model of the Articular Disc of the Temporomandibular Joint. *Experimental Mechanics*, *56*(7), 1169–1177. https://doi.org/10.1007/s11340-016-0161-2
Crandall, J. R., Bose, D., Forman, J., Untaroiu, C. D., Arregui-Dalmases, C., Shaw, C. G., & Kerrigan, J. R. (2011). Human surrogates for injury biomechanics research. *Wiley Online Library*, *24*(3), 362–371. https://doi.org/10.1002/ca.21152
Duma, S. M., Schreiber, P. H., McMaster, J. D., Crandall, J. R., & Bass, C. R. (2002). Fracture tolerance of the male forearm: The effect of pronation versus supination. *Proceedings of the Institution of Mechanical Engineers, Part D: Journal of Automobile Engineering*, *216*(8), 649–654. https://doi.org/10.1177/095440700221600803
Forman, J. L., Lopez-Valdes, F. J., Duprey, S., Bose, D., Del Pozo De Dios, E., Subit, D., Gillispie, T., Crandall, J. R., & Segui-Gomez, M. (2015). The tolerance of the human body to automobile collision impact - A systematic review of injury biomechanics research, 1990-2009. *Accident Analysis and Prevention*, *80*, 7–17. https://doi.org/10.1016/j.aap.2015.03.004
Frampton, R., Morris, A., Thomas, P., & Bodiwala, G. (1997). An overview of upper extremity injuries to car occupants in Uk vehicle crashes. *Proceedings of the International Research Council on the Biomechanics of Injury Conference*, *25*(September), 37–51.
Garcia, C. A., Hoffman, S. L., Hastings, M. K., Klaesner, J. W., & Mueller, M. J. (2008). Effect of metatarsal phalangeal joint extension on plantar soft tissue stiffness and thickness. *Foot*, *18*(2), 61–67. https://doi.org/10.1016/j.foot.2007.12.002
Gefen, A., & Haberman, E. (2007). Viscoelastic properties of ovine adipose tissue covering the gluteus muscles. *Journal of Biomechanical Engineering*, *129*(6), 924–930. https://doi.org/10.1115/1.2800830
Gottsauner-Wolf, F., Grabowski, J. J., Chao, E. Y. S., & An, K. -N. (1995). Effects of freeze/thaw conditioning on the tensile properties and failure mode of bone-muscle-bone units: A biomechanical and histological study in dogs. *Journal of Orthopaedic Research*, *13*(1), 90–95. https://doi.org/10.1002/jor.1100130114
Hendriks, F. M., Brokken, D., van Eemeren, J. T. W. M., Oomens, C. W. J., Baaijens, F. P. T., & Horsten, J. B. A. M. (2003). A numerical-experimental method to characterize the non-linear mechanical behavior of human skin. *Skin Research and Technology*, *9*(3), 274–283. https://doi.org/10.1034/j.1600-0846.2003.00019.x
Jernigan, M. V., Rath, A. L., & Duma, S. M. (2005). Severe upper extremity injuries in frontal automobile crashes: The effects of depowered airbags. *American Journal of Emergency Medicine*, *23*(2), 99–105. https://doi.org/10.1016/j.ajem.2004.02.045
Leonard, K. C., Worden, N., Boettcher, M. L., Dickinson, E., & Hartstone-Rose, A. (2022). Effects of freezing and short-term fixation on muscle mass, volume, and density. *Anatomical Record*, *305*(1), 199–208. https://doi.org/10.1002/ar.24639
Miller-Young, J. E., Duncan, N. A., & Baroud, G. (2002). Material properties of the human calcaneal fat pad in compression: Experiment and theory. *Journal of Biomechanics*, *35*(12), 1523–1531. https://doi.org/10.1016/S0021-9290(02)00090-8
Mitchell, S., Payne, T., & Bibb, R. (2013). Design of human surrogates for the study of biomechanical injury: A review. In *Critical Reviews in Biomedical Engineering* (Vol. 41, Issue 1, pp. 51–89). https://doi.org/10.1615/CritRevBiomedEng.2013006847

This paper is a student paper from the 19th Injury Biomechanics Symposium and is published in a special issue of SAE International Journal of Transportation Safety.
It is preliminary work, has not been peer reviewed, and should not be cited because it is a work in progress.

Oliver, W., & Pharr, G. M. (1992). An improved technique for determining hardness and elastic modulus using load and displacement sensing indentation experiments. *Journal of Materials Research*, *7*(6), 1564–1583. https://doi.org/10.1557/jmr.1992.1564

Pintar, F. A., & Yoganandan, N. (2002). Dynamic bending tolerance of the human forearm. *Traffic Injury Prevention*, *3*(1), 43–48. https://doi.org/10.1080/15389580210520

Shinohara, M., Sabra, K., Gennisson, J. L., Fink, M., & Tanter, M. L. (2010). Real-time visualization of muscle stiffness distribution with ultrasound shear wave imaging during muscle contraction. *Muscle and Nerve*, *42*(3), 438–441. https://doi.org/10.1002/mus.21723

Shoham, N., & Gefen, A. (2016). The biomechanics of fat: From tissue to a cell scale. In *Structure-Based Mechanics of Tissues and Organs* (pp. 79–92). Springer US. https://doi.org/10.1007/978-1-4899-7630-7_5

Sun, Z., Gepner, B. D., Lee, S. H., Rigby, J., Cottler, P. S., Hallman, J. J., & Kerrigan, J. R. (2021). Multidirectional mechanical properties and constitutive modeling of human adipose tissue under dynamic loading. *Acta Biomaterialia*, *129*, 188–198. https://doi.org/10.1016/j.actbio.2021.05.021

Sun, Z., Lee, S. H., Gepner, B. D., Rigby, J., Hallman, J. J., & Kerrigan, J. R. (2021). Comparison of porcine and human adipose tissue loading responses under dynamic compression and shear: A pilot study. *Journal of the Mechanical Behavior of Biomedical Materials*, *113*. https://doi.org/10.1016/j.jmbbm.2020.104112

Van Loocke, M., Simms, C. K., & Lyons, C. G. (2009). Viscoelastic properties of passive skeletal muscle in compression-Cyclic behaviour. *Journal of Biomechanics*, *42*(8), 1038–1048. https://doi.org/10.1016/j.jbiomech.2009.02.022

Van Sligtenhorst, C., Cronin, D. S., & Wayne Brodland, G. (2006). High strain rate compressive properties of bovine muscle tissue determined using a split Hopkinson bar apparatus. *Journal of Biomechanics*, *39*(10), 1852–1858. https://doi.org/10.1016/j.jbiomech.2005.05.015

Ward, S. R., & Lieber, R. L. (2005). Density and hydration of fresh and fixed human skeletal muscle. *Journal of Biomechanics*, *38*(11), 2317–2320. https://doi.org/10.1016/j.jbiomech.2004.10.001

Zhang, M., Zheng, Y. P., & Mak, A. F. T. (1997). Estimating the effective Young's modulus of soft tissues from indentation tests - Nonlinear finite element analysis of effects of friction and large deformation. *Medical Engineering and Physics*, *19*(6), 512–517. https://doi.org/10.1016/S1350-4533(97)00017-9

This paper is a student paper from the 19th Injury Biomechanics Symposium and is published in a special issue of SAE International Journal of Transportation Safety.
It is preliminary work, has not been peer reviewed, and should not be cited because it is a work in progress.